Bulletin of Electrical Engineering and Informatics
Vol. 3, No. 4, December 2014, pp. 293~154
ISSN: 2089-3191

Determination of Melting Layer Boundaries and Attenuation Evaluation in Equatorial Malaysia at Ku-Band

Abayomi Isiaka O. Yussuff*[1], Nor Hisham Haji Khamis[2]
[1]Dept. of Electronic & Computer Engineering, Lagos State University, Nigeria
[2]Dept. of Communication Engineering, Universiti Teknologi Malaysia, Malaysia
*Corresponding author, e-mail: ayussuff@yahoo.com[1], hisham@fke.utm.my[2]

Abstract

Upsurge in bandwidth demand in recent times for real-time data transmission have put serious constraints on satellite communication channels, leading to congestion of the lower frequency bands; necessitating migration to higher bands (Ku, Ka and V) with attendant problems such as signal fading, depolarization and attenuation due to presence of hydrometeors. There is need to separately account for attenuation due to the melting layer along the earth-space microwave links. One year data from ground-based S-band meteorological radar sourced from Kluang station of the Malaysian Meteorological Department was processed to build the vertical reflectivity of rain profile for UTM, Malaysia. Results from this work suggested that the effects of the melting layer on signal attenuation at Ku-band can be quite significant in the tropical and equatorial regions. It was estimated to be 13.36 dB and 15.44 dB at 0.01% of the time exceeded using Laws-Parsons and Marshall-Palmer regression coefficients, respectively. Furthermore, it was observed that ITU-R. P.618-11 model largely under-estimated the attenuation along the slant-paths because of its failure to account for attenuation due to the melting layer in its formulation by its assumption of constant rain rate; thus rendering it unsuitable for rain attenuation predictions in the tropics.

Keywords: *Break-point attenuation, Rain rates, Stratiform rain, Melting layer, 0^0C Isotherm height*

1. Introduction

The lack of direct knowledge of the microphysical and associated radiative properties of certain precipitation particles like melting hydrometeors, which have an important radiative impact in stratiform regions, have led to subjective assumptions in the retrieval algorithms; neglecting the effect of the melting layer in the retrieval has been shown to lead to a possible overestimation of the precipitation for light stratiform rain [1]. The total path attenuation is found by assuming constant rain up to the bottom of the melting layer and adding the attenuation excess of the melting layer. When the $0°C$ level is higher, the relative influence of the melting layer decreases and vice versa [2], [3]. Furthermore, failure to account for attenuation due to the melting layer will result in poor attenuation predictions and link budget analysis for satellite communications in the tropical and equatorial regions because of their peculiar rainfall precipitations. Therefore, attenuation due to the melting layer should be included in the ITU-P.618-11 Recommendations to adequately account for signal loss due to the melting layer. As shown in the results of this work, the ITU-R. P.618-11 [4] model which is presently the most popular and widely adopted attenuation prediction method for satellite communication, largely under-estimated the attenuation along the slant-path because of its failure to include melting layer attenuation in its formulations.

From Dissanayake's model [5], Equation (1) gives the relationship between the rain rate R (mm/h) and the specific attenuation in the melting layer, α_m.

$$\alpha_m = aR^b \quad \text{(dB/km)} \tag{1}$$

Received October 9, 2014; Revised November 15, 2014; Accepted November 30, 2014

The thickness of the melting layer, D_m was taken to be 0.5 km and the path length through the melting layer, $L_m = 0.5/\sin\theta$ (km). Where the elevation angle is θ, the path length was restricted to a maximum value of 10km. Thus, melting layer attenuation A_m is given by Equation (2).

$$A_m = \alpha_m L_m (dB);\ L_m \leq 10\,\text{km} \quad (2)$$

The attenuation produced by the melting ice particles within the melting layer can reach significant levels; especially for low elevation angle Earth-space links [5]. Although the specific attenuation in the melting layer is not always significantly larger than that in the rain region underneath it, rain attenuation modelling, being largely semi-empirical, normally accounts for melting effects for moderate to high rainfall rates. Therefore, a separate account of the melting layer is required for low rain rates [5], [6].

In order to properly characterize the bright-band, stratiform rain events must be present. Convective rainfalls have narrow horizontal area and are associated with extensive rainfall rates, larger rain drops and height. They are produced by cumulus clouds [7]. Stratiform rains on the other hand are characterized by light intensity; widespread rainfalls with smaller rain drop sizes. They are brought about by stratus clouds [7]. Since rain height is highly correlated with signal attenuation and co-channel interference due to rain drop scattering, proper characterization of the melting layer from the vertical reflectivity profile (VRP) built from radar observations in stratiform rain events is essential. Also, rain height distribution can be used to investigate the mechanisms responsible for variations in the attenuation distributions at any station of interest. Apart from the ambiguity in estimating the attenuation due to the melting layer, other sources of errors in slant path attenuation predictions include complexity of the rainfall structure along slant-path and difficulties encountered in empirically relating rain and isotherm heights in the tropicalregions, due to insufficient database [8].

The melting layer is the region where solid ice transits into rain as they fall; lying just below the 0^oC isotherm height. This transformation subsequently leads to increase in the hydrometeors reflectivity as a result of the differences in the dielectric constants of water and ice; which consequently manifests in the bright-band signature seen in radar measurements [9-12]. More so, the depolarization effect of the melting layer can be quite significant because of the non-sphericity of the melting ice crystals' shape [13]. Furthermore, the melting layer is a major factor responsible for the problems being encountered in quantification and modelling of earth-to-space microwave signal propagation attenuations, link budget analysis and equipment designs.

In spite of the general supposition that attenuation due to the melting layer are insignificant enough to be ignored, recent researches has shown that the effect of melting layer on signal attenuation is not after all negligible [14], [15], especially for weak rain rates [16] and in the Q/V/W frequency bands [17]. Attenuation due to the melting layer (containing melting hydrometeors) has received less interest over the years when compared to rain and dry snow attenuations. This is because the melting layer is more difficult to compute than the other parameters. X-band radar observations have shown that bright-band attenuation is three to five times the specific attenuation computed for rain only (without considering melting layer) [15]. Scattering, above and within the melting layer and absorption within and below the melting layer are key factors responsible to signal extinction in hydrometeors. Another problem is the paucity of Earth-Satellite rain attenuation database for use in rain propagation studies in the tropical (and equatorial)regions of the world [8], [18-21].

International Telecommunication Union-Recommendation (ITU-R) P.618-11 rain attenuation model [4] is the most widely accepted international method for the prediction of rain effects on satellite communication systems. The predicted slant-path attenuation exceeded for 0.01% of an average year is:

$$A_{0.01} = \gamma_{0.01} L_{eff}\ \text{dB} \quad (3)$$

Where is the effective slant-path length; $A_{0.01}$ and $\gamma_{0.01}$ are attenuation and specific attenuation at 0.01% of time respectively.

The predicted attenuation exceeded for other percentages $\%p$ of an average year may be obtained from the value of $A_{0.01}$ by using the following extrapolation [4]:

$$A_{P\%} = A_{0.01}\left(\frac{p}{0.01}\right)^{-[0.655+0.033\ln p-0.045\ln A_{0.01}-z\sin\theta(1-p)]}\text{dB} \quad (4)$$

Where p is the percentage probability of interest and z is given by:

$$For \quad p \geq 1.0\%, z = 0 \quad (5)$$

$$For\ p<1.0\%, z=\begin{cases} 0;\ for\ /\phi/\geq 36^0 \\ z=-0.005(/\phi/-36)\ \ for\ \theta\geq 25^0 and /\phi/<36^0 \\ z=-0.005(/\phi-36/)+1.8-4.25\sin\theta,\ \ for\ \theta<25^0 and /\phi/<36^0 \end{cases} \quad (6)$$

The modified ITU-R (or breakpoint) model by [22], [23] is based on the premise that the accumulation time factor at the breakpoints is an invariant in the tropics. Also, for elevation angles less than 60^0 and at high rain rates, multiple rain cells were observed to intersect along the slant path [22]. The attenuation exceedance is predicted by two expressions very much similar to the ITU-R model; with one expression each for stratiform and convective rainfall types (Equations (10) and (11) respectively). The breakpoint attenuation exceedances, P_{AB} and rain rate exceedances, P_{RB} are related as [22]:

$$P_{AB} = 2.14\ P_{RB} \quad (7)$$

This gives an approximate value of P_{AB} as 0.021% for tropical regions of the world as shown in Figure 1.

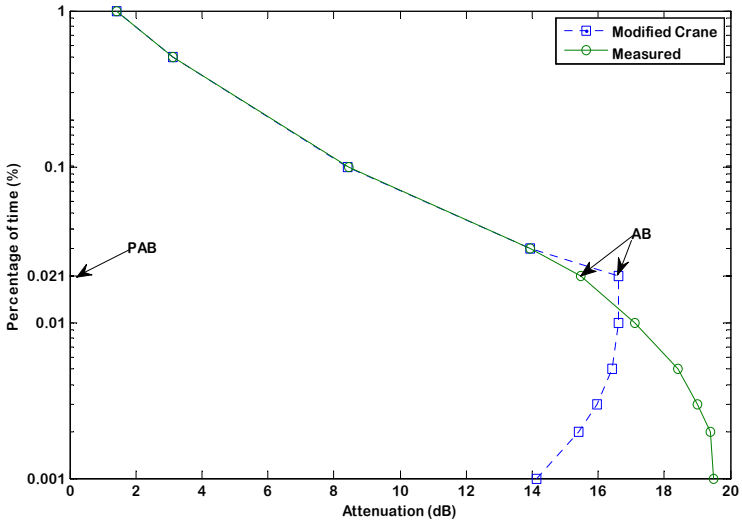

Figure 1. Measured and Breakpoint Attenuation exceeded for UTM, Malaysia at 12 GHz

$$A_B = kR_B^{\alpha} * Leff * C_f \text{ dB} \quad (8)$$

Where, correction factor

$$C_f = \begin{cases} -0.002|\theta|^2 + 0.175|\theta| - 2.3 ; 40° \le \theta < 60° \\ 1 ; \theta \ge 60° \end{cases} \quad (9)$$

Where k and α are both frequency dependent parameters; A_B and R_B are attenuation and rain rate at breakpoints, respectively. The attenuation predictions for P% of time are:
For stratiform rainfall,

$$A_P = A_B \left(\frac{p - 0.011}{0.01}\right)^{-[0.655 + 0.033\ln(p - 0.011) - 0.045\ln A_B - z\sin\theta(0.989 - p)]} dB \quad (10)$$

For convective rainfall,

$$A_P = A_B \left(\frac{p - 0.011}{0.021}\right)^{-0.5[0.655 + 0.033\ln(p^2) - 0.045\ln A_B - z\sin\theta(0.989 - p)]} dB \; ; \; p \le 0.021 \quad (11)$$

Equations (10) and (11) are modified ITU-R P.618-10 of equation (4).

Most countries in the temperate regions have reasonably sufficient terrestrial rain attenuation data; while on the contrary, very little data is available for slant-path links for purposes of design and budget analysis in the tropical and equatorial regions. If the bright-band was not recognized, it can result in serious under-estimation of total link budget analysis for satellite communication [15], [17], especially in the tropical and equatorialregions of the world.

2. Research Method

Universiti Teknologi Malaysia (1.56^{o}N, 103.64^{o}E) is 62 km from the Malaysian Meteorological Department's Kluang radar station (2.02^{o}N, 103.38^{o}E); with an azimuthal angle of 169^o. This one year measurement data were taken between December 1, 2006 and November 30, 2007. The classification of the rain events were evaluated by radar operators at the Malaysian Meteorological Department with the minimum amount of the rain rate that the radar can detect using the widely accepted Marshall-Palmer [24] empirical relationship of the radar reflectivity factor. This is expressed in as in Equation (12).

$$Z = aR^b \quad (\text{mm}^6\text{m}^{-3}) \quad (12)$$

where the values for a and b are 200 and 1.6 respectively.

The Kluang radar is a 3-D RAPIC system that utilizes two scan modes. These are the plan position indicator (PPI) and rain height indicator (RHI). The Kluang meteorological radar isa vertically-polarized pulse radar, operating in the S-band (2.8 GHz) frequency range; with sensitivity time control (STC) of 230 km and a bandwidth of 2^o. The transmitting and receiving antennas are both 3.66 m parabolic reflectors types, installed at an altitude of 88.1 m above the mean sea level.Minimum and maximum search windows were set to 1 and 15 km respectively; hence the elevation angles used in this work are 1.1°, 1.9°, 3.3°, 5.8°, 7.7°, 10.3° and 13.6°, with an additional elevation angle of 18.1° to cater for possible tropical thunderstorm rain events that could lead to unexpected updrafts.

After filtering out the Kluang radar data from the other stations contained in the raw data, the contents of the selected eight volumetric elevation angles were subsequently extracted from the filtered data, using MATLAB program codes. In doing these, only data scanned at a higher resolution of 500 meters were extracted fromKluang radar data. Since the raw data is encoded in ASCII, the extracted data is decoded and subsequently the VRP is plotted from the eight selected elevation angles recorded through the 169^o RHI azimuthal scan range. Finally, various melting layer parameters, such as rain and $0°C$ isotherm heights and bright-band thickness are obtained.

3. Results and Discussions

Shown in Figure 2 are the mean VRP plots from Kluang ground-based meteorological radar from one year observation.

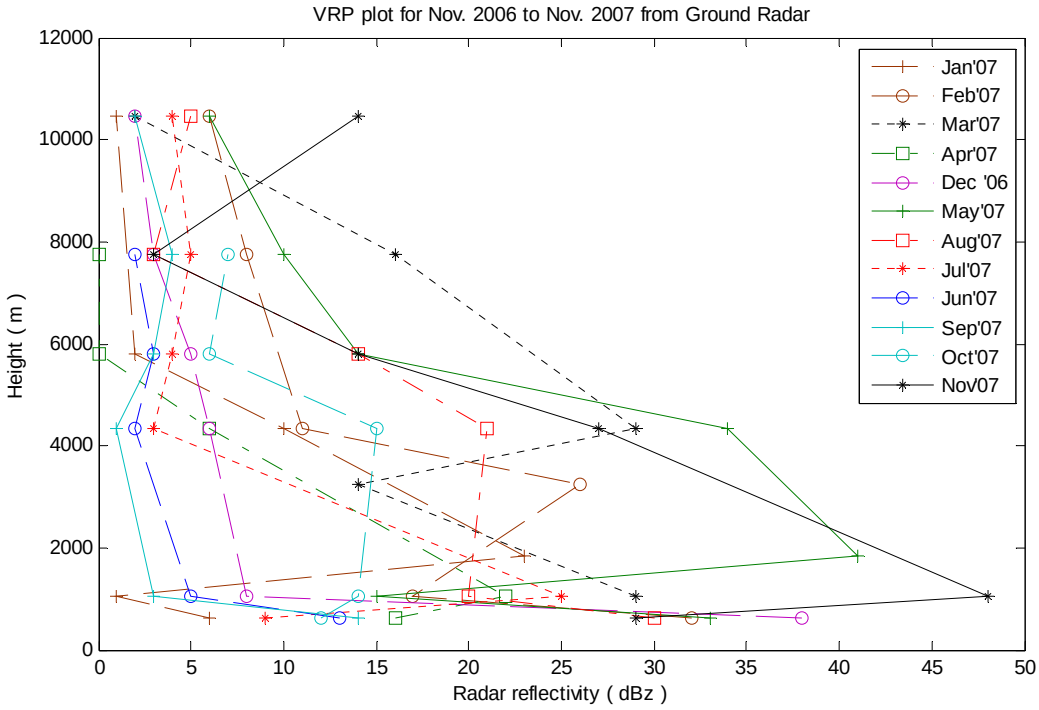

Figure 2. Vertical reflexivity profiles from radar measurements for UTM, Malaysia

Each of these VRPs was built from the mean heights and mean radar reflectivity values for each of the corresponding months. Malaysia annually experience two seasonal monsoon events and two inter-monsoon seasons [25]. The seasonal monsoon events are the North-East monsoon (December to March), influenced by an air mass originating from the South China Sea and the South-West monsoon (June to September). It is brought about by the heavy air mass movement from the Indian Ocean. These two monsoon events results in two rainy and two dry seasons annually. The inter-monsoon periods are between April-May and October-November, respectively.

It is observed that the 0^{o}C isotherm and rain heights are at their peak in the months of March and September 2007, coinciding with the end of the two monsoons. Equally, these parameters are observed to be lowest in February, April, July and October of 2007. Similarly, the bright-band is thickest in February and August 2007. February and August are the months preceding the end of both monsoon seasons (March and September), thus showing seasonal dependence [12]. These parameters have been found to be directly correlated to signal attenuation along the earth-space link.

Furthermore, the rain and 0^{o}C isotherm heights correlation plot from ITU-R P.839-3 [28] and that obtained from this radar observation is shown in Figure 3.

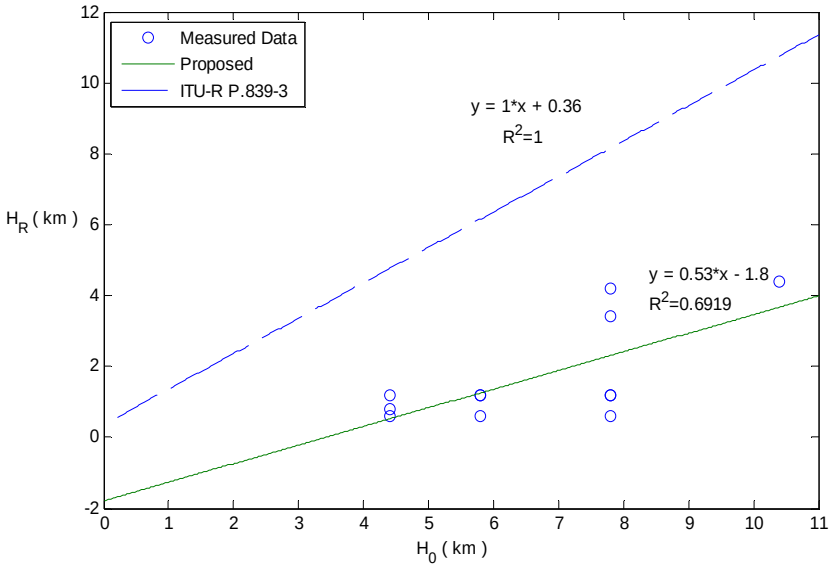

Figure 3. H_R against H_0 for ITU-R and proposed plots for UTM, Malaysia

Equation (13) presents the mathematical relationship between rain and 0°C isotherm heights.

$$H_R = 0.53\, H_0 - 1.8 \text{ km} \quad (13)$$

Where H_R and H_0 are rain and $0^0 C$ isotherm heights respectively.

This plot was arrived at by synthesizing the ITU-R P.839-3 model with H_0 from the measured data. From Figure 3, it is clear that ITU-R P.839-3 model is largely theoretical (with a correlation factor, R^2 of 1).

Figures 4 and 5 showed the effects of the melting layer on the total attenuation experienced along the earth-space link. The attenuation due to the melting layer was computed using Equations (1) and (2) from Dissanayake [5] melting layer model. The regression coefficients for the computation of specific attenuations for Marshall and Palmer, M-P [24] and Laws and Parsons, L-P [26] empirical radar relationships at 0°C for 12 GHz frequency link are obtained from [27].

From Figures 4 and 5, the attenuations due to the 3.03 km thick melting layer [29] using regression coefficients from [26] and [24] at 0.01% of the time exceeded are 13.36 dB and 15.44 dB respectively. These are quite significant when compared to the measurement value of 17.12 dB due to rain alone, at the same percentage of time exceeded. This result shows that there is under-estimation of total link budget for satellite communication when the effects of attenuation due to the melting layer are not accounted for. This could result in poor attenuation predictions.This is corroborated by [15], [17].

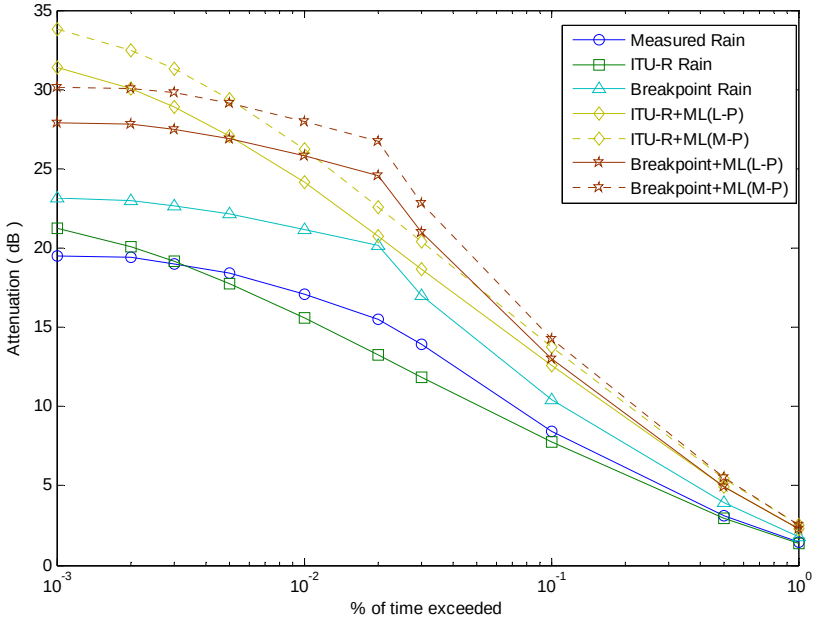

Figure 4. Rain attenuation exceeded for UTM, Malaysia at 12 GHz

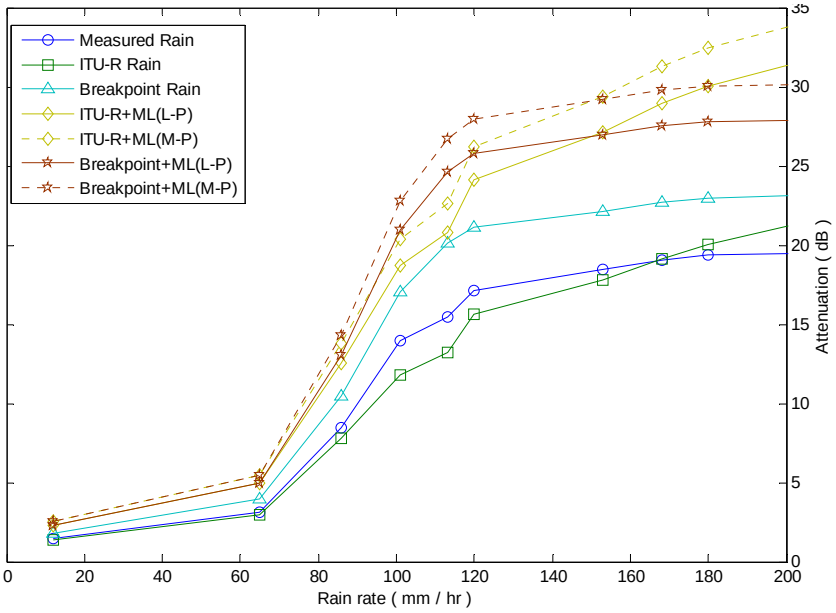

Figure 5. H_R against H_0 for ITU-R and proposed plots for UTM, Malaysia

Table 1 is the statistical percentage and root mean square errors for the purposes of comparison between the ITU-R and breakpoint (BP) model.

From the evaluation procedures adopted for comparison of prediction methods by the Recommendations ITU-R P.311-13 [30], the best prediction method is one that produces the smallest values of the statistical parameters. Therefore, when the presence of the melting layer is taken into account, the breakpoint model using the L-P regression coefficients produced the best results for $0.001\% \leq p \leq 0.005\%$ and $p = 1.0\%$ of the time exceeded, while a combination of

the ITU-R model with the L-P coefficients showed better performance between $0.01\% = p \le 0.5\%$ of the time.

The idealization of ITU-R P.839-3 modelby not taking in to account seasonal variations; and the assumption of constant rain height up to the $0°C$ isotherm may be responsible for the variations between the results of ITU-R model and those from actual measurement data; thus, rendering the ITU-R P.839-3 model unsuitable for earth-space attenuation predictions for tropical and equatorial locations (like Malaysia).

Table 1. Percentage Errors and RMS Comparison

Parameter	Prediction Models	Time percentage (%p)									
		0.001	**0.002**	**0.003**	**0.005**	**0.01**	**0.02**	**0.03**	**0.1**	**0.5**	**1.0**
Mean	**ITU-R**	0.0089	0.0036	0.0008	-0.0036	-0.0089	-0.0144	-0.0152	-0.0082	-0.0049	-0.0048
	Breakpoint	0.0185	0.0184	0.0194	0.0203	0.0236	0.0302	0.0221	0.0235	0.0259	0.0262
	ITU-R+L-P	0.0609	0.0552	0.0522	0.0471	0.041	0.0342	0.034	0.0485	0.0588	0.0611
	ITU-R+M-P	0.0733	0.0676	0.0646	0.0593	0.0531	0.0461	0.0462	0.0627	0.0751	0.0781
	BP+L-P	0.043	0.0434	0.0448	0.0462	0.0507	0.0591	0.0502	0.0541	0.0596	0.0609
	BP+M-P	0.0545	0.055	0.0567	0.0584	0.0635	0.0727	0.0636	0.0688	0.0758	0.0779
Std. Dev.	**ITU-R**	0.0022	0.0078	0.0086	0.0078	0.0021	0.0116	0.0125	0.0025	0.0071	0.0071
	Breakpoint	0.0138	0.0139	0.0126	0.011	0.0048	0.0194	0.0068	0.0045	0.0118	0.0124
	ITU-R+L-P	0.0344	0.0228	0.0141	0.0176	0.0291	0.0368	0.037	0.0132	0.0306	0.0348
	ITU-R+M-P	0.0396	0.0276	0.0192	0.0168	0.0313	0.0409	0.0409	0.0113	0.0428	0.0479
	BP+L-P	0.0286	0.028	0.0257	0.0231	0.0098	0.0287	0.012	0.0163	0.0297	0.0324
	BP+M-P	0.0359	0.035	0.0323	0.0291	0.015	0.0322	0.0146	0.0219	0.0387	0.0425
RMS	**ITU-R**	0.0091	0.0069	0.0085	0.0069	0.0091	0.0185	0.0197	0.0079	0.0051	0.0053
	Breakpoint	0.0124	0.0121	0.0148	0.017	0.0241	0.0359	0.021	0.0239	0.0285	0.029
	ITU-R+L-P	0.07	0.0597	0.0541	0.0436	0.0288	0.0138	0.0146	0.0466	0.0663	0.0704
	ITU-R+M-P	0.0833	0.073	0.0674	0.0569	0.0429	0.0212	0.0214	0.0637	0.0864	0.0916
	BP+L-P	0.0321	0.0331	0.0366	0.04	0.0497	0.0657	0.0488	0.0565	0.0666	0.069
	BP+M-P	0.041	0.0425	0.0466	0.0506	0.0617	0.0795	0.0619	0.0722	0.0852	0.0887

4. Conclusion

There is need to properly and separately account for signal attenuations due to hydrometeors such as rain and the melting layer along the earth-space microwave links, especially in the tropics. To realize this, it is necessary to adequately characterize the bright-band in order to eliminate any ambiguity in the estimation of the attenuation due to the melting layer. Results from this work suggest that the quantifications of bright-band parameters in the tropical (and equatorial) regions are influenced by seasonal and latitudinal variations. Breakpoint prediction model with L-P regression coefficients showed best performance for $0.001\% \le p \le 0.005\%$ and $p = 1.0\%$ of the time exceeded. However, ITU-R model also with L-P coefficients showed better results between $0.01\% = p \le 0.5\%$ of the time. Again, ITU-R models (ITU-R. P.839-3 and ITU-R.P.618-11) were found to be unsuitable for prediction of attenuation due to the melting layer in the tropical and sub-tropical stations. This is partly because they fail to account the existence of the melting layer; and therefore mostly either over-estimated or under-estimated the measurements.

References

[1] Brown ST, Ruf CS. Validation and development of melting layer models using constraints by active/passive microwave observations of rain and the wind-roughened ocean surface. *Journal of Atmospheric and Ocean Technology.* 2007; 24: 543–563.

[2] Klaassen W. Radar observations and simulation of the melting layer of precipitation. *Journal of the atmospheric sciences.* 1988; 45(24): 3741-3753.

[3] Klaassen, W. *Attenuation and reflection of radio waves by a melting layer of precipitation*. IEE Proceedings. 1990; 137H(I): 39-44.

[4] ITU-R. P. 618-11, *Propagation Data and Prediction Methods Required for the Design of Earth-Space Telecommunications Systems*, Recommendation ITU-R P Series.Geneva: IEEE Press; 2013.

[5] Dissanayake A, Allnutt J, Haidara F. A prediction model that combines rain attenuation and other propagation impairments along earth-satellite paths. *Antennas and Propagation, IEEE Transactions*. 1997; 45(10): 1546-1558.

[6] Botta G, Aydin K, Verlinde J. Modeling of microwave scattering from cloud ice crystal aggregates and melting aggregates: A new approach. *IEEE Geosci and Remote Sens. Lett.* 2010: 7: 572–576.

[7] Lam HY, Din J, Capsoni C, Panagopoulos AD. *Stratiform and Convective rain Discrimination for Equatorial Region*. Proceedings of 2010 IEEE SCOReD. 2010: 112-116.

[8] Ajayi GO, Odunewu PA. *Some Characteristics of the Rain Height in a Tropical Environment*. Antennas and Propagation, 1989. ICAP 89, Sixth International Conference on (Conf. Publ. No. 301). IET, Coventry. 1989: 80-82.

[9] Das S, Maitra A. (2011). *Some melting layer characteristics at two tropical locations inIndian region*, General Assembly and Scientific Symposium, 2011 XXXth URSI. IEEE. 2011: 1-4.

[10] Konstantinos P, Melina I, Dimitrios C. *Comparison of radar reflectivity calculations to satellite measurements across the melting layer of precipitation*, General Assembly and Scientific Symposium, 2011 XXXth URSI IEEE. 2011: 1-4.

[11] Raymond L, et al. *Improved Modelling of Propagation and Backscattering of Millimeter waves in the Melting Layer*. IEEE National Conference on Antennae and Propagation. 1999: 160-163.

[12] Fabry A Bellon, Zawadzki II. *Long Term Observations of the Melting Layer Using Vertically Pointing Radars MW-101*. Report. Vol. 65, McGill University, Canada. 1-65.1994.

[13] Sarkar T, Das S, Maitra A. Effects of melting layer on Ku-band signal depolarization. *Journal of Atmospheric and Solar-Terrestrial Physics*. 2014: 1-21. doi: http://dx.doi.org/10.1016/j.jastp.2014.06.006

[14] Nebuloni R, Capsoni C. *Laser attenuation by falling snow, Communication Systems*. Networks and Digital Signal Processing, CNSDSP. 6th International Symposium. 2008: 265-269.

[15] Olivier P, Frédéric M, Sauvageot H. Effects of Melting Layer in Airborne Meteorological X-Band Radar Observations, *IEEE Transactions on Geoscience and Remote Sensing*. 2012; 50(6): 2318-2324.

[16] Takahashi N, Awaka J. *Introduction of a melting layer model to a rain retrieval algorithm for microwave radiometers*. Geoscience and Remote Sensing Symposium, IGARSS'05 Proceedings. 2005; 5: 3404-3409.

[17] Luini L, Capsoni C. *Performance Evaluation of Satellite Communication Systems Operating in the Q/V/W Bands*. Report. Politecnico di Milano, Dipartimento di Elettronica e Informazione, Italy. 2-37.2013.

[18] Adetan O, Afullo TJ. Raindrop size distribution and rainfall attenuation modeling in equatorial and subtropical Africa: the critical diameters, *Annals of telecommunications-annales des telecommunications*. 2014:1-13.

[19] Adhikari A, Bhattacharya A, Maitra A. Rain-induced scintillations and attenuation of Ku-band satellite signals at a tropical location. *Geoscience and Remote Sensing Letters, IEEE*. 2012; 9(4): 700-704.

[20] Mandal BK, Bhattacharyya D, Kang S. Attenuation of Signal at a Tropical Location with Radiosonde Data Due to Cloud. *International Journal of Smart Home*. 2014; 8(1): 15-22.

[21] Rahim SKA, Rahman TA, Tan KG, Reza AW. Microwave signal attenuation over terrestrial link at 26 GHz in Malaysia. *Wireless Personal Communications*. 2012; 67(3): 647-664.

[22] Bryant GH, Adimula I, Riva C, BrussaardG. Rain attenuation statistics from rain cell diameters and heights. *International journal of satellite Communications*. 2001; 19(3): 263-283.

[23] Ramachandran V, Kumar V. Modified rain attenuation model for tropical regions for Ku-Band signal. *International Journal of Satellite Communications and Networking*. 2007; 25(1): 53-67.

[24] Marshall JS, Palmer WMK. The distribution of raindrops with size. *Journal of meteorology*. 1948; 5(4): 165-166.

[25] Kozu T, Reddy KK, Mori S, Thurai M, Ong JT, Rao DN, Shimomai T. Seasonal and diurnal variation of raindrop size distribution in Asian monsoon region. *Journal of Applied Meteor. Soc. Japan*. 2006; 84A: 195–209.

[26] Laws JO, Parsons DA. The Relationship of Raindrop Size to Intensity. *Transactions - America Geophysical Union*. 1943; 24: 452–460.

[27] Zhang W, Moayeri N. *Power-Law Parameters of Rain Specific Attenuation*. Report, National Institute of Standards and Technology, IEEE. 1-8. 1999.

[28] ITU-R. P.839-3. *Rain height model for prediction methods*, Recommendation ITU-R P Series.Geneva: IEEE Press; 2001.
[29] Yussuff, A. I. O. Characterization of bright-band in a tropical station for satellite communications.Ph.D. Thesis. Dept. of Communications Engineering, Universiti Teknologi Malaysia. 2014.
[30] ITU-R P.311-13. *Acquisition, presentation and analysis of data in studies of tropospheric propagation*, Recommendation, ITU-R Radio Propagation Series.Geneva: IEEE Press; 2009.